VIP pH-Sensitive Microgels Very Important Paper

DOI: 10.1002/anie.201402254

The Compressibility of pH-Sensitive Microgels at the Oil–Water Interface: Higher Charge Leads to Less Repulsion**

*Karen Geisel, Lucio Isa, and Walter Richtering**

Abstract: *pH-responsive microgels are unique stabilizers for stimuli-sensitive emulsions that can be broken on demand by changing the pH value. However, recent experiments have indicated that electrostatic interactions play a different role to that in conventional Pickering emulsions. The influence of charges on the interactions between microgels at the oil–water interface is now described. Compression isotherms of microgels with different charge density and architecture were determined in a Langmuir trough, and counter-intuitive results were obtained: Charged microgels can be compressed more easily than uncharged microgels. The compressibility of microgels is thus not determined by direct Coulomb repulsion. Instead, the different swelling of the microgels in the charged and the uncharged states is proposed to be the key parameter.*

It has recently been discovered that responsive microgels can be used as unique stabilizers for stimuli-sensitive emulsions. Microgels are cross-linked, solvent-swollen, and thus soft polymeric particles that adapt their size and structure according to their local environment. They are surface-active, arrange around droplets, prevent coalescence, and produce highly stable emulsions. Furthermore, responsiveness imparts extra functionalities to microgel-stabilized emulsions, and droplets can be broken on demand by changing external parameters, such as the temperature or the pH value.[1–13] These special properties are relevant for many applications, for example, in biocatalysis.[6]

On first sight, microgel-stabilized emulsions are similar to Pickering emulsions, which are stabilized by hard particles. However, the softness of microgels leads to distinct differences; for example, the microgels are strongly deformed,[14] and the softer the microgels are, the better they stabilize emulsions.[12] Furthermore, the stability of the emulsion does not only depend on the surface properties of the microgels, but can also be controlled by their internal properties, especially in core–shell microgels.[5]

A prominent example of a responsive microgel is poly(*N*-isopropylacrylamide) (P(NIPAM)). This polymer has a lower critical solution temperature of 32 °C in aqueous solution, and P(NIPAM) microgels undergo a volume phase transition from a swollen to a collapsed state at this temperature.[15,16]

P(NIPAM) microgels lower the interfacial tension between water and air[17,18] as well as that between water and oil.[19,20] Several aspects influence the stability of microgel-stabilized emulsions, including the spatial distribution of charged co-monomers inside the particle and the crosslink density.[12,13] Differences to rigid colloidal particles have previously been discussed.[4,21]

The incorporation of ionic co-monomers into P(NIPAM) microgels leads to additional responsiveness towards the pH value.[22,23] Charged microgels swell more strongly than uncharged microgels because of the osmotic pressure of the counterions; they also experience long-range Coulomb repulsion.[24] However, emulsions that are stabilized by charged microgels do not exhibit typical charge effects, such as an attraction between differently charged droplets. It was even shown that oppositely charged droplets that are covered by microgels do not coalesce when they are mixed.[3]

Furthermore, direct electron microscopy of the microgel-covered interface with freeze-fracture shadow-casting (FreSCa) cryogenic scanning electron microscopy (cryo-SEM)[25] revealed the three-dimensional structure of the microgels at the interface. The particles are strongly deformed at the interface and protrude very little into the oil phase.[26] The degree of deformation and the protrusion height do not depend on the charge of the microgels.

Extracting information on the interaction between particles at the surface of emulsion droplets is a rather demanding task, as curvature effects might not be negligible. Therefore, it is important to investigate flat interfaces as model systems for curved interfaces, such as in droplets. A defined and controlled flat interface can be achieved in a Langmuir trough, where the influence of compression on the particle layer can be investigated in detail.

Herein, we present surprising findings on the behavior of microgels at the oil–water interface during compression in a Langmuir trough. In particular, we used charged and uncharged microgels with uniform and non-uniform distributions of charges to investigate the influence of electrostatic interactions on the compressibility. Compression isotherms of microgel monolayers at the decane–water interface were recorded. We will show below that increasing the number of charges in the microgel does not lead to stronger repulsion.

[*] Dipl.-Chem. K. Geisel, Prof. Dr. W. Richtering
Physical Chemistry, RWTH Aachen University
Landoltweg 2, 52056 Aachen (Germany)
E-mail: richtering@rwth-aachen.de
Prof. Dr. L. Isa
Laboratory for Interfaces, Soft Matter and Assembly
Department of Materials, ETH Zurich
Vladimir Prelog Weg 5, 8093 Zürich (Switzerland)

[**] L.I. acknowledges the SNSF (PZ00P2_142532/1 and PP00P2_144646/1) for financial support and the Electron Microscopy Centre of the ETH Zurich (EMEZ) for technical support. K.G. and W.R. acknowledge financial support from the Deutsche Forschungsgemeinschaft within the Sonderforschungsbereich SFB 985 "Functional Microgels and Microgel Systems".

Supporting information for this article is available on the WWW under http://dx.doi.org/10.1002/anie.201402254.

Instead, charged microgels can be compressed more easily than uncharged ones.

The microgel that was used for a first set of experiments is a poly(*N*-isopropylacrylamide-*co*-methacrylic acid) (P(NIPAM-*co*-MAA)) microgel. It is thermo- as well as pH-sensitive, but we focused on the pH sensitivity in this study, and all experiments were performed at 20 °C. The methacrylic acid is protonated at pH 3 and deprotonated at pH 9, so that charges are introduced to the microgel at high pH values. This is represented by an increase in the electrophoretic mobility from $(-0.09 \pm 0.01) \times 10^{-8}\,m^2\,V^{-1}\,s^{-1}$ at pH 3 to $(-0.70 \pm 0.03) \times 10^{-8}\,m^2\,V^{-1}\,s^{-1}$ at pH 9. The charges induce a swelling of the microgels that is due to the osmotic pressure of the counterions. The hydrodynamic diameter in water increases from $d_w = 276 \pm 3$ nm at pH 3 to $d_w = 362 \pm 4$ nm at pH 9. The crosslink density of the microgels is not uniform throughout the particle, but decreases towards the outside. Therefore, microgels possess a core–corona structure with a higher polymer density in the core.[12,14,26,27]

In the following sections, we compare compression isotherms (surface pressure vs. specific area) of the microgel in the uncharged state at pH 3 and the charged state at pH 9 at the decane–water interface.

Compression isotherms of different amounts of the P(NIPAM-*co*-MAA) microgels that are spread at the interface in the uncharged and in the charged state are shown in Figure 1. For each pH value, several individual isotherms, which correspond to different initial microgel concentrations at the interface, are shown. These individual isotherms can be combined to form master curves by normalizing the trough area to the amount of microgel at the interface. The non-normalized isotherms are given in the Supporting Information (Figure S1 and S2).

The normalized isotherms for different charge states qualitatively show a similar trend. The surface pressure vanishes at low concentration and low compression, and it is independent of the area. At this point, the microgels at the interface are highly diluted and do not interact with each other. Upon compression, the microgel concentration at the interface increases, as a smaller area is available per microgel. The particles start to interact, and the surface pressure rises steeply under compression. Further compression leads to the formation of a pseudo-plateau, at which the surface pressure is almost independent of the area again. This first pseudo-plateau at $\pi = 30\,mN\,m^{-1}$ can be assigned to a coexistence of two phases, similar to the expanded and condensed liquid states of monolayers of classical surfactants.[28] In microgel systems, we propose that the expanded liquid state corresponds to the coronas of the microgels being in contact, whereas in the condensed liquid state, the coronas become compressed or overlap with each other (see below for comments on possible mechanisms). This pseudo-plateau is followed by a second rise in surface pressure when the microgels are compressed further. The final plateau is reached at a high compression of $\pi \approx 35\,mN\,m^{-1}$. At this point, the microgels cannot get closer to each other, and the formation of multilayers, the desorption of particles from the interface, or buckling of the microgel layer are likely to occur. Nakahama et al. measured compression isotherms of P(NIPAM) microgel monolayers at the air–water interface, and the surface pressure also showed a two-step increase during compression. They attributed this to a change in interaction, from soft repulsion when the corona is compressed to stronger steric repulsion when the coronas overlap, and the highly crosslinked core is compressed.[29]

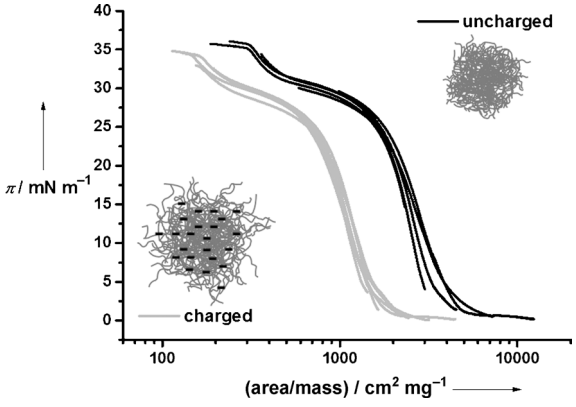

Figure 1. Compression isotherms of different amounts of the P(NIPAM-*co*-MAA) microgel in the charged and uncharged state at the decane–water interface. The area is normalized to the mass of microgel that is placed at the interface. The schematic representations of the microgels show their pH-dependent swelling and the decreasing crosslink density from the center to the periphery. The size ratio is approximately to scale, and counterions are omitted. For non-normalized isotherms, see Figures S1 and S2.

Differences between charged and uncharged particles can be seen in the specific area for the onsets of the increase in surface pressure and the formation of the plateaus. The surface pressure starts to rise at higher surface concentrations (i.e., smaller area per mass) in the charged state as compared to the uncharged state, and the plateau also starts at higher concentrations. The charges in the microgel change the behavior under compression, and the microgels can be compressed further before a change in surface pressure is detected. This is in striking contrast to the behavior of pH-sensitive microgels in bulk, where long-range electrostatic repulsion is observed.[24] Instead, the introduction of charges has a different effect on microgels sitting at an oil–water interface. This effect is stronger than direct Coulomb repulsion.

The different behavior under compression is even more surprising because we have seen in an earlier study, using FreSCa cryo-SEM imaging, that the size and degree of the flattening of the microgels at the oil–water interface after adsorption and self-assembly is very similar ($d_i = 559 \pm 49$ nm in the uncharged state and $d_i = 534 \pm 14$ nm in the charged state).[26] Therefore, there is an inconsistency between the image analysis and the isotherms: The microgel size at the interface is similar, but the isotherms of the charged and the uncharged microgels show differences in the specific area where the surface pressure starts to change. The latter can be illustrated by first shifting the isotherm of the charged microgel to match the curve of the uncharged microgel (Figure 2) and then comparing this shift with the size of the microgels at the interface (Figure 3).

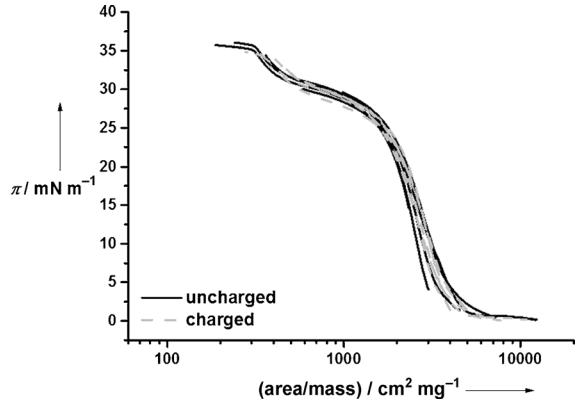

Figure 2. Compression isotherms of the P(NIPAM-*co*-MAA) microgel after the isotherm of the charged microgel had been shifted to larger areas.

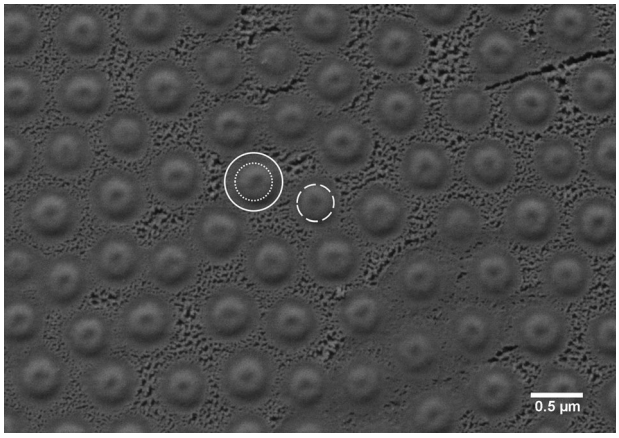

Figure 3. FreSCa cryo-SEM image of the P(NIPAM-*co*-MAA) microgel in the uncharged state at the heptane–water interface. Microgels are seen from the heptane side after fracturing. The core–corona structure of the uncharged microgels at the interface is visible ($d = 559$ nm, closed and dotted circles), and the apparent size of the charged microgels (derived from the compression isotherms) is depicted ($d = 357$ nm, dashed circle).

Shifting the isotherm of the charged microgel by a factor of 2.43 to higher specific areas leads to superimposition with the isotherm of the uncharged microgel ($2.43 \times$ "charged" = "uncharged"). The observation that the isotherms at high and low pH values can be overlapped indicates that the general processes during compression do not change for charged microgels. Nevertheless, the presence of charges changes the properties of the microgel so that it can be compressed further before an increase in surface pressure is observed. Thus, the charged microgels have a lower effective area and a smaller effective size.

The different effective areas of charged and uncharged microgels at the interface can be compared with the structure of microgels as observed in FreSCa cryo-SEM micrographs. The microgels reveal a distinct core–corona morphology, and the dotted and closed circles in Figure 3 illustrate core and corona, respectively. The dashed circle in Figure 3 indicates the size that is obtained when the entire area of core and corona is divided by 2.43 (which corresponds to the shift of the isotherms). The smaller effective size of the charged microgel as calculated from the shift of the isotherms resembles the size of the core of the uncharged microgel.

We considered three mechanisms by which the microgels can react to compression. First, their size could decrease. The particles show a core–corona structure at the interface, and the size of the corona can decrease during compression of the microgel layer. However, the size of the corona was found to be independent of charge.[26]

A second possible mechanism can be related to the fact that the main part of the charged and the uncharged microgels is placed in the aqueous phase. Charged microgels swell more strongly in the aqueous phase than their uncharged counterparts. Furthermore, the presence of a charged microgel will lead to an image charge in the oil phase. This can drag the microgels more into the water phase, which results in smaller protrusion into the oil phase. A difference in protrusion height for the charged and the uncharged microgels was not detected by FreSCa cryo-SEM, but this could be due to the very small protrusion into the oil phase and limitations of the technique.[26] It is thus possible that small deviations in the protrusion height facilitate an overlap of the coronas during compression of the charged microgels. The particles can then get closer to each other before changes in the surface pressure are detected.

Third, the chains at the surface of the microgels can interpenetrate during compression. In this context, it is important to recall the structure of microgels in bulk again. Charged microgels in bulk are swollen and soft and possess a fuzzy surface with dangling polymer chains. In contrast, uncharged microgels are denser. Even though FreSCa cryo-SEM images did not indicate an influence of the charge on the microgel size,[26] it is possible that the density of the polymer chains in the corona is different in the charged and uncharged states. Such density differences are hardly detectable by SEM. A higher softness of the charged microgels would facilitate microgel compression. As swelling and softness are more pronounced for charged microgels than for uncharged microgels, they can penetrate more easily.

The analysis of the compression isotherms of the P(NIPAM-*co*-MAA) microgel discussed above leads to the conclusion that Coulomb interactions are not the main parameter influencing the isotherms. Instead, the swelling properties of the microgels in different charge states seem to play a major role in their compression at the interface. It can thus be expected that a microgel that does not show Coulomb interactions but pH-dependent swelling behaves similar to the P(NIPAM-*co*-MAA) microgel. For this reason, we prepared a second microgel with an additional, pure P(NIPAM) shell on the P(NIPAM-*co*-MAA) core. A much smaller amount of charges is present at the surface of the second microgel because of the P(NIPAM) shell. The electrophoretic mobility changes less with the pH value than for the first microgel (from $(-0.05 \pm 0.02) \times 10^{-8}\,m^2\,V^{-1}\,s^{-1}$ at pH 3 to $(-0.22 \pm 0.02) \times 10^{-8}\,m^2\,V^{-1}\,s^{-1}$ at pH 9). The pH-dependent swelling of the microgel is restricted by the non-pH-sensitive shell,[30,31] but the hydrodynamic diameter in water still increases from $d_w = 378 \pm 9$ at pH 3 to $d_w = 400 \pm 14$ nm at pH 9. This shows

that the pH-dependent swelling that is due to the osmotic pressure of the counterions is still present, and that this microgel has a much lower surface charge than the P(NIPAM-*co*-MAA) microgel.

The normalized compression isotherms of the second microgel in the charged and the uncharged state follow the same trend as the isotherms of the P(NIPAM-*co*-MAA) microgels (Figure 4). The same two-step increase in the surface pressure is observed during compression. Again, the isotherm of the charged microgel is found at lower areas than the one of the uncharged microgel, which is in agreement with the observations for the P(NIPAM-*co*-MAA) microgel. Furthermore, the isotherm in the charged state can be shifted to match the isotherm in the uncharged state (Figure 4).

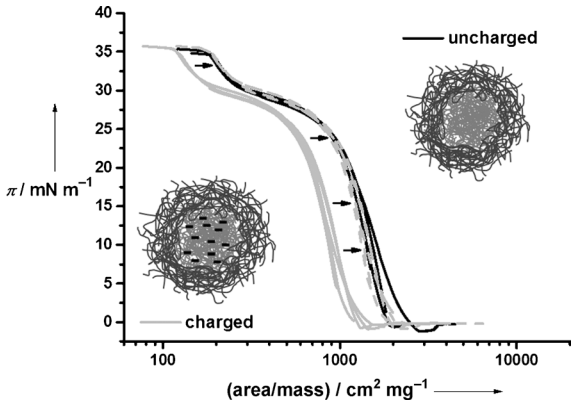

Figure 4. Compression isotherms of different amounts of the second microgel in the charged and in the uncharged state at the decane–water interface. The area is normalized to the mass of microgel that is located at the interface. The isotherm of the charged microgel can additionally be shifted to larger areas (dashed grey line). Schematic representations of the microgels show their morphology and that the pH-dependent swelling of the core is restricted by the shell. The size ratio is approximately to scale, and counterions are omitted. For non-normalized isotherms, see Figures S3 and S4.

The diameter of the microgels at the interface was again determined by FreSCa cryo-SEM imaging, and, in analogy to the first microgel, no significant differences in the deformation were found between uncharged and charged state.[26] The shift in the isotherms (Figure 4) corresponds to a 1.54-fold increase in area (Figure 5). The difference between the apparent size of the charged microgel and the size at the interface is smaller than for the P(NIPAM-*co*-MAA) microgel. This is most likely due to the corset effect of the shell in the second microgel;[32] however, the pH influence is still clearly visible in Figure 4.

In conclusion, we have found an unexpected influence of charges on the compression of P(NIPAM-*co*-MAA) microgels: Charged microgels can be compressed further than the uncharged microgels. Therefore, the compression isotherms are not directly influenced by charge repulsion. The apparent particle size for the charged microgels can be derived from a comparison of the compression isotherms in the charged and the uncharged state. This size is significantly smaller than the size of the deformed microgel, that is core and corona,

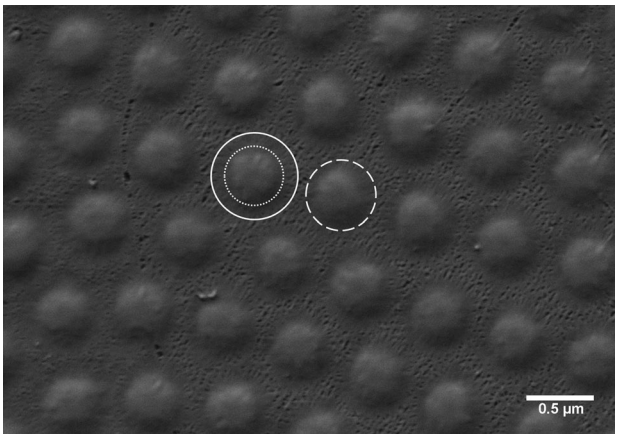

Figure 5. FreSCa cryo-SEM image of the second microgel in the uncharged state at the heptane–water interface, seen from the heptane side after fracturing. The core–corona structure of the uncharged microgels is depicted by dotted (core) and closed (corona; $d = 642$ nm) circles. The apparent size of the charged microgel as derived from the shift in the compression isotherms in Figure 4 is also shown (dashed circle, $d = 518$ nm).

which was determined by FreSCa cryo-SEM. However, it is close to the size of the cores alone. We suggest that the internal structure of individual particles, for example their crosslink density profile and their response to changes in the pH value, play an important role in defining the compression behavior at different charge levels. This hypothesis is supported by the comparison of two microgels with different charge distributions. Even though charges in the second microgel are mainly located in the core, swelling was observed at high pH values, and the compression isotherms differed, similar to what was observed for the first homogeneously charged microgel. It can thus be stated that the charges in microgels do not influence the compressibility of a microgel monolayer in a straightforward manner, that is, directly by charge repulsion, but instead indirectly, through different swelling properties that arise from the presence of the charges themselves.

In contrast to our findings, it was shown that Coulomb repulsion plays an important role for rigid micrometer-sized silica particles under compression at the oil–water interface.[33] Theoretical calculations also showed that charge repulsion can dominate over capillary interaction (i.e., attraction) when hard particles at the oil–water interface are considered.[34] Our findings thus illustrate that the behavior of soft microgels at oil–water interfaces is distinctly different from that of hard particles.

Experimental Section

The microgel synthesis was done by standard precipitation polymerization with a surfactant and has already been described in detail elsewhere.[26] A detailed description of the experimental procedures can be found in the Supporting Information. In brief, compression isotherms were recorded on a Langmuir trough equipped with two movable barriers. A platinum plate was placed parallel to the barriers, and the change in surface pressure was recorded with a Wilhelmy balance. A defined amount of aqueous microgel dispersion was

placed directly at the decane–water interface, and the compression was performed after an equilibration time of 1 h with a speed of 10 mm min^{-1}. Isopropylalcohol was added to the microgel dispersion to facilitate spreading at the interface.

Received: February 11, 2014
Published online: March 28, 2014

Keywords: compression isotherms · electrostatic interactions · interfaces · pH-sensitive microgels · Pickering emulsions

[1] B. Brugger, W. Richtering, *Langmuir* **2008**, *24*, 7769.
[2] B. Brugger, B. A. Rosen, W. Richtering, *Langmuir* **2008**, *24*, 12202.
[3] T. Liu, S. Seiffert, J. Thiele, A. R. Abate, D. A. Weitz, W. Richtering, *Proc. Natl. Acad. Sci. USA* **2012**, *109*, 384.
[4] W. Richtering, *Langmuir* **2012**, *28*, 17218.
[5] S. Schmidt, T. Liu, S. Rütten, K.-H. Phan, M. Möller, W. Richtering, *Langmuir* **2011**, *27*, 9801.
[6] S. Wiese, A. C. Spiess, W. Richtering, *Angew. Chem.* **2013**, *125*, 604; *Angew. Chem. Int. Ed.* **2013**, *52*, 576.
[7] Z. Li, T. Ngai, *Colloid Polym. Sci.* **2011**, *289*, 489.
[8] T. Ngai, H. Auweter, S. H. Behrens, *Macromolecules* **2006**, *39*, 8171.
[9] T. Ngai, S. H. Behrens, H. Auweter, *Chem. Commun.* **2005**, 331.
[10] M. Destribats, V. Lapeyre, E. Sellier, F. Leal-Calderon, V. Ravaine, V. Schmitt, *Langmuir* **2012**, *28*, 3744.
[11] M. Destribats, V. Lapeyre, E. Sellier, F. Leal-Calderon, V. Schmitt, V. Ravaine, *Langmuir* **2011**, *27*, 14096.
[12] M. Destribats, V. Lapeyre, M. Wolfs, E. Sellier, F. Leal-Calderon, V. Ravaine, V. Schmitt, *Soft Matter* **2011**, *7*, 7689.
[13] M. Destribats, M. Wolfs, F. Pinaud, V. Lapeyre, E. Sellier, V. Schmitt, V. Ravaine, *Langmuir* **2013**, *29*, 12367.
[14] B. Brugger, S. Ruetten, K.-H. Phan, M. Moeller, W. Richtering, *Angew. Chem.* **2009**, *121*, 4038; *Angew. Chem. Int. Ed.* **2009**, *48*, 3978.
[15] H. G. Schild, *Prog. Polym. Sci.* **1992**, *17*, 163.
[16] R. Pelton, *Adv. Colloid Interface Sci.* **2000**, *85*, 1.
[17] J. Zhang, R. Pelton, *Langmuir* **1999**, *15*, 8032.
[18] Y. Cohin, M. Fisson, K. Jourde, G. G. Fuller, N. Sanson, L. Talini, C. Monteux, *Rheol. Acta* **2013**, *52*, 445.
[19] Z. Li, K. Geisel, W. Richtering, T. Ngai, *Soft Matter* **2013**, *9*, 9939.
[20] C. Monteux, C. Marliere, P. Paris, N. Pantoustier, N. Sanson, P. Perrin, *Langmuir* **2010**, *26*, 13839.
[21] V. Schmitt, V. Ravaine, *Curr. Opin. Colloid Interface Sci.* **2013**, *18*, 532.
[22] T. Hoare, R. Pelton, *Langmuir* **2004**, *20*, 2123.
[23] S. Zhou, B. Chu, *J. Phys. Chem. B* **1998**, *102*, 1364.
[24] P. S. Mohanty, W. Richtering, *J. Phys. Chem. B* **2008**, *112*, 14692.
[25] L. Isa, F. Lucas, R. Wepf, E. Reimhult, *Nat. Commun.* **2011**, *2*, 438.
[26] K. Geisel, L. Isa, W. Richtering, *Langmuir* **2012**, *28*, 15770.
[27] M. Stieger, W. Richtering, J. S. Pedersen, P. Lindner, *J. Chem. Phys.* **2004**, *120*, 6197.
[28] V. M. Kaganer, H. Möhwald, P. Dutta, *Rev. Mod. Phys.* **1999**, *71*, 779.
[29] K. Nakahama, K. Fujimoto, *Langmuir* **2002**, *18*, 10095.
[30] C. D. Jones, L. A. Lyon, *Macromolecules* **2003**, *36*, 1988.
[31] I. Berndt, J. S. Pedersen, P. Lindner, W. Richtering, *Langmuir* **2006**, *22*, 459.
[32] I. Berndt, J. S. Pedersen, W. Richtering, *Angew. Chem.* **2006**, *118*, 1769; *Angew. Chem. Int. Ed.* **2006**, *45*, 1737.
[33] R. Aveyard, J. H. Clint, D. Nees, V. N. Paunov, *Langmuir* **2000**, *16*, 1969.
[34] K. D. Danov, P. A. Kralchevsky, *J. Colloid Interface Sci.* **2010**, *345*, 505.

